

## OPEN ACCESS

## EDITED BY

Inna Lermontova,  
Leibniz Institute of Plant Genetics and  
Crop Plant Research (IPK), Germany

## REVIEWED BY

Anne Bagg Britt,  
University of California, Davis,  
United States  
Cécile Raynaud,  
UMR9213 Institut des Sciences des  
Plantes de Paris Saclay (IPS2), France

## \*CORRESPONDENCE

Ales Pecinka  
pecinka@ueb.cas.cz

## SPECIALTY SECTION

This article was submitted to  
Plant Genetics, Epigenetics and  
Chromosome Biology,  
a section of the journal  
Frontiers in Plant Science

RECEIVED 19 August 2022

ACCEPTED 14 November 2022

PUBLISHED 12 December 2022

## CITATION

Vladejić J, Yang F,  
Dvořák Tomaštková E, Doležel J,  
Pelecěk JJ and Pecinka A (2022)  
Analysis of BRCT5 domain-containing  
proteins reveals a new component of  
DNA damage repair in Arabidopsis.  
*Front. Plant Sci.* 13:1023358.  
doi: 10.3389/fpls.2022.1023358

## COPYRIGHT

© 2022 Vladejić, Yang, Dvořák  
Tomaštková, Doležel, Pelecěk and  
Pecinka. This is an open-access article  
distributed under the terms of the  
[Creative Commons Attribution License  
\(CC BY\)](https://creativecommons.org/licenses/by/4.0/). The use, distribution or  
reproduction in other forums is  
permitted, provided the original  
author(s) and the copyright owner(s)  
are credited and that the original  
publication in this journal is cited, in  
accordance with accepted academic  
practice. No use, distribution or  
reproduction is permitted which does  
not comply with these terms.

# Analysis of BRCT5 domain-containing proteins reveals a new component of DNA damage repair in Arabidopsis

Jovanka Vladejić<sup>1</sup>, Fen Yang<sup>1,2</sup>, Eva Dvořák Tomaštková<sup>1</sup>,  
Jaroslav Doležel<sup>1</sup>, Jan J. Polecěk<sup>3</sup> and Ales Pecinka<sup>1,2\*</sup>

<sup>1</sup>Institute of Experimental Botany (IEB), Czech Acad Sci, Centre of the Region Haná for Biotechnological and Agricultural Research (CRH), Olomouc, Czechia, <sup>2</sup>Department of Cell Biology and Genetics, Faculty of Science, Palacký University, Olomouc, Czechia, <sup>3</sup>National Centre for Biomolecular Research (NCBR), Faculty of Science, Masaryk University, Brno, Czechia

The integrity of plant genetic information is constantly challenged by various internal and external factors. Therefore, plants use a sophisticated molecular network to identify, signal and repair damaged DNA. Here, we report on the identification and analysis of four uncharacterized Arabidopsis BRCT5 DOMAIN CONTAINING PROTEINs (BCPs). Proteins with the BRCT5 domain are frequently involved in the maintenance of genome stability across eukaryotes. The screening for sensitivity to induced DNA damage identified BCP1 as the most interesting candidate. We show that BCP1 loss of function mutants are hypersensitive to various types of DNA damage and accumulate an increased number of dead cells in root apical meristems upon DNA damage. Analysis of publicly available *sog1* transcriptomic and SOG1 genome-wide DNA binding data revealed that *BCP1* is inducible by gamma radiation and is a direct target of this key DNA damage signaling transcription factor. Importantly, *bcp1* plants showed a reduced frequency of somatic homologous recombination in response to both endogenous and induced DNA damage. Altogether, we identified a novel plant-specific DNA repair factor that acts downstream of SOG1 in homology-based repair.

## KEYWORDS

DNA damage repair, genome stability, BRCT domain, BRCT5 domain, homologous recombination, Arabidopsis

## Introduction

Genome stability is constantly threatened by internally and externally-induced DNA damage (Razqallah, 2008; Chatterjee and Walker, 2017). Among others, the presence of damaged DNA negatively affects DNA replication, transcription, and cell cycle progression. Therefore, living organisms developed a sophisticated safeguarding

system that recognizes various types of DNA damage, signals their presence, and activates specific molecular effectors that repair the damaged site. This prevents the occurrence of potentially deleterious mutations. Once the repair is completed, the halted cellular processes are restarted and continued. Numerous studies demonstrated that DNA damage repair is essential for the normal growth and fertility of plants, similar to other organisms (Manova and Gruszka, 2015; Nisa et al., 2019). However, despite a generally high degree of evolutionary conservation of the eukaryotic DNA repair system, several unique DNA repair factors evolved in plants (Yoshiyama et al., 2013b; Hu et al., 2016).

Depending on the type of DNA damage, specific DNA repair pathways are activated. A common and highly toxic type of lesion is DNA double-strand break (DSB), which may be generated by external or internal factors. Its persistence in the genome may lead to a loss of genetic information, structural genome changes, and even cell death. The DSB repair begins with a recognition of the damaged site by the MRN (MRE11-RAD50-NBS1) complex and phosphorylation of histone variant H2A.X to produce gamma-H2A.X. This stimulates the binding of the transcription factor Breast cancer type 1 susceptibility protein (BRCA1), followed by signaling through Ataxia Telangiectasia Mutated (ATM) and/or ATM- and RAD3-related (ATR) kinases. The kinase activity of ATM and/or ATR activates the p53 transcription factor at the sites of DNA damage in metazoa and its functional homolog SUPPRESSOR OF GAMMA RADIATION 1 (SOG1) in plants (Preuss and Britt, 2003; Seton-Rogers, 2006; Yoshiyama et al., 2009; Hafner et al., 2019). During the following steps, these transcription factors orchestrate various responses, including pausing of the cell cycle, promotion repair by non-homologous end-joining (NHEJ) or homologous recombination (HR), or (in extreme cases) cell death. In contrast with the error-prone NHEJ, HR represents an error-free mechanism where an intact DNA molecule homologous to the damaged site is used as a template for repair (Heyer et al., 2010). Although the mechanism of HR is studied in great detail across the major branches of the tree of life, not all molecular factors taking place in this process are known.

A prominent group of proteins associated with cell cycle regulation and DNA damage repair contains the BRCA1 C-Terminus (BRCT) domain (Bork et al., 1997), which consists of approximately 100 amino acids and mediates protein-protein interactions by binding to the phosphate groups (Yu et al., 2003). Later studies in animals and yeasts suggested several structurally distinct types of BRCT domains (Wan et al., 2016). The best-studied examples of plant BRCT domain-containing proteins are the BRCA1 and its homolog BREAST CANCER ASSOCIATED RING 1 (BARD1). Both proteins are required for normal levels of somatic HR in plants, and their loss of function mutants are hypersensitive to DNA damage (Trapp et al., 2011). A

conspicuous type of BRCT domain is the BRCT5 that was found in budding and fission yeast proteins Rtt107 and Brc1, respectively, and in human protein NSE5/SLF1 (Williams et al., 2010; Li et al., 2012; Räschle et al., 2015). These proteins represent species-specific cofactors involved in the loading of the evolutionary conserved DNA damage repair complex Structural maintenance of chromosomes 5/6 (SMC5/6) to chromatin (Leung et al., 2011; Räschle et al., 2015; Oravcová et al., 2019). However, none of the currently known plant SMC5/6 complex interactors contains this domain. Another example of BRCT5 domain-containing protein includes human Pax2 transactivation domain-interacting protein (PTIP) that performs ATM-dependent activation of p53 and thus promotes DSB repair in mammals (Yan et al., 2011). PTIP also lacks a functional homolog in plants. Therefore, BRCT5 domain proteins represent a little understood group in plants.

Our study demonstrates that analyzing plant proteins carrying BRCT5 domain-containing is an attractive route toward discovering new players involved in the control of plant genome stability. Thus we performed *in silico* identification of Arabidopsis BRCT5 DOMAIN CONTAINING PROTEINs (BCPs). Subsequently, loss of function mutants of four genes was characterized by the expression pattern and hypersensitivity to DNA damage. The most promising candidate BCP1 was analyzed as to its role in HR-based repair.

## Materials and methods

### Plant materials and growth conditions

Unless stated otherwise, all *Arabidopsis thaliana* (Arabidopsis) genotypes used in this study had Columbia (Col-0) background. T-DNA lines used in this study were: GK\_301C08 (*bcp1-1*), SALK\_001578C (*bcp1-2*), SALK\_022790 (*bcp1-3*), GK\_076D08 (*bcp2-1*), SALK\_111173C (*bcp3-1*), SALK\_038422 (*bcp4-1*), and SALK\_123114C (*smc6b-1*). T-DNA mutant lines were obtained from the SALK institute (Alonso et al., 2003) and GABI-Kat (Kleinboelting et al., 2012) via the European Arabidopsis Stock Centre (NAS). Double mutants were generated by crossing homozygous single mutants and analyzing progeny in F2 generation by PCR-based genotyping for both mutations. HR reporter lines B11 in the C24 background (Swoboda et al., 1994) and IC9C (Puchta et al., 1995; Molinier et al., 2004) were crossed with *bcp1-1*. The resulting hybrids were grown into F4 generation and selected by PCR for double homozygous lines. The oligonucleotides used for genotyping are listed in Supplementary Table 1.

Plants used for phenotyping, seed generation, and crossing were grown in climate-controlled phytotron under long-day conditions (at 16 h light, 150  $\mu\text{mol m}^{-2} \text{s}^{-1}$  intensity, 19°C during the day; 8 h at 18°C during the night). *In vitro* plant

cultivation was done in an air-conditioned phytochamber with a long day regime (16h light,  $150 \mu\text{mol m}^{-2} \text{s}^{-1}$ , 21°C, 8h dark, 19°C).

## Basic local alignment search tool and BRCT5 domain structure comparisons

New Arabidopsis BRCT5 domain-containing proteins were identified by the BLAST search (Altschul et al., 1990) using the fission yeast *Schizosaccharomyces pombe* Brc1 (*SpBrc1*) and human *Homo sapiens* NSE5 (*HsNSE5*) proteins against the *Arabidopsis thaliana* database (taxid: 3702). The retrieved BRCT5 domain sequences were manually aligned, and their AlphaFold structural models (Varadi et al., 2022) were compared.

## Molecular cloning, plant transformation, and GUS assays

To develop the promoter-reporter line, a region 2000 bp upstream of the *BCP1* transcription start site (*ProBCP1*) was amplified by PCR and cloned by Gateway Technology (ThermoFisher Scientific; Cat. nos.: 11789100, 12538120) into *pDONR207* (Invitrogen) and then recombined into the binary vector *pKGWFS7.0*, containing *uidA* gene encoding  $\beta$ -glucuronidase (GUS). Plasmids carrying the *ProBCP1::GUS* fusion were transformed into *Agrobacterium tumefaciens* strain GV3101. Transformation of *Arabidopsis* Col-0 was performed using the floral dip method. (Zhang et al., 2006). The selection of transformed plants in T1 generation was carried out on a medium containing 100  $\mu\text{g/ml}$  kanamycin (Sigma-Aldrich, Cat. no. 60615). Resistant plants were transferred to soil for seed production. The following generation (T2) of plants was selected based on the activation of the *GUS* reporter gene. The oligonucleotides used for genotyping or cloning are listed in Supplementary Table 1.

The expression pattern of *BCP1* in highly dividing vegetative tissues, as well as the change of expression under DNA damage stress, was examined by using a *ProBCP1::GUS* reporter line. Plants grown for seven days on a solid medium were transferred for 24 h to liquid  $\frac{1}{2}$  MS medium with or without 10  $\mu\text{M}$  mitomycin C (MMC, Cat. no. M0503), a genotoxic agent causing intrastrand DNA crosslinks. Following the treatments, plants were stained by GUS histochemical staining. GUS solution containing 10 mM EDTA (Sigma-Aldrich, Cat. no. E5134), 2 mM potassium ferrocyanide (Lachema, Cat. no. 68 4514), 2 mM potassium ferricyanide (Lachema), 100 mM disodium phosphate (Penta, Cat. no. 15150), 100 mM monosodium phosphate (Lachema, Cat. no. 68 4639), 0.1% Triton X-100 (Sigma-Aldrich, Cat. no. T8787) and 2 mM X-Gluc (Thermo Scientific, Cat. no. R0852) was prepared as described in (Baubec et al., 2009). Seedlings were transferred to 5 ml tubes and infiltrated with GUS staining solution under a vacuum. After five to ten minutes, the vacuum was

released and tubes were placed at 37°C overnight. Subsequently, the GUS staining solution was removed and plants were cleared by incubation in 70% ethanol (v/v) at 37°C. Ethanol was changed 3 times, and after the last change, plants were left overnight at 4°C. Pictures were taken under a stereo-microscope (Olympus SZX16) and fluorescent microscope (Olympus BX60).

For the analysis of *BCP1* expression in the reproductive tissues, inflorescences were fixed in 90% (v/v) acetone and incubated for 45 min at -20°C. Acetone was then removed, and samples were washed three times with 100 mM phosphate buffer, pH 7.2. After washing, the flowers were infiltrated with GUS staining solution under a vacuum for 10 min and left overnight at 37°C. The next morning the solution was removed, and samples were washed shortly with phosphate buffer and cleared in chloral hydrate solution containing eight parts chloral hydrate (Sigma-Aldrich, Cat. no. 23100) two parts water, and one part glycerol (Sigma-Aldrich, Cat. no. G516). Flowers were mounted on the microscope slide and dissected in the same solution. Pictures were taken under a stereo-microscope (Olympus SZX16) and fluorescent microscope (Olympus BX60).

## Root sensitivity assays

For root sensitivity assays, surface sterilized and stratified seeds were grown on  $\frac{1}{2}$  MS growth medium with 0.6% agar (w/v) and 1% sucrose (w/v). Seeds were sterilized in 70% ethanol (v/v) for 5 min, followed by 8% sodium hypochlorite solution (v/v) for 6-10 min, and washed 3 times in sterile water. Seeds were stratified for 48h in 0.1% agarose solution (w/v) at 4°C in the dark. Stratified seeds were evenly distributed on Petri dishes containing  $\frac{1}{2}$  MS medium (mock) or  $\frac{1}{2}$  MS medium supplemented with 10  $\mu\text{M}$  MMC (Sigma-Aldrich, Cat. no. M0503), 20 nM camptothecin (CPT; Sigma-Aldrich, Cat. no. C9911), 20  $\mu\text{M}$  zebularine (Sigma-Aldrich, Cat. no. Z4775), or 50 nM bleomycin (Sigma-Aldrich, Cat. no. 203408-M). Plants grown for seven days in a horizontal position were then carefully pulled off the medium using tweezers and laid flat on a plate with agar. The length of the primary root was measured using the ImageJ plugin SmartRoot (Lobet et al., 2011). Experiments were performed in three biological replicates with typically 20 plants per replicate (minimum of 11 plants in one replicate). Statistical significance was tested with One-way ANOVA with posthoc Tukey HSD in Minitab.

## Cell death assays

Sterilized and stratified seeds were grown vertically on plates with  $\frac{1}{2}$  MS medium with 0.8% agar (w/v) for five days and then transferred into liquid  $\frac{1}{2}$  MS medium for a 24 h treatment. Mock samples were grown in pure liquid  $\frac{1}{2}$  MS medium, while treated plants had medium supplemented with 10  $\mu\text{M}$  MMC. Following the treatment, seedlings were stained with 10  $\text{mg}\cdot\text{mL}^{-1}$  propidium

iodide solution (Sigma) on glass microscope slides. Visualization and photography were performed using Leica confocal microscope TCS SP8 (Leica, Wetzlar, Germany) and HC PL APO CS2 20x/0.75 DRY objective equipped with Leica LAS-X software with Leica Lightning module laser scanning confocal microscope (Leica). At least 13 plants for each group were analyzed. The means of the three replicates are depicted. Statistical significance was tested with Kruskal-Wallis H-test with *post hoc* Conover-Iman test of multiple comparisons using rank sums with Benjamini-Hochberg procedure in R 4.2.1 (R Core Team, 2018).

## Homologous recombination assays

The B11, B11 *bcp1-1*, IC9C, and IC9C *bcp1-1* plants were grown on ½ MS medium with or without (mock) 1 µM MMC under sterile conditions. Ten days-old seedlings were histochemically stained using GUS as described above. Plants were transferred to a Petri dish containing ethanol and examined using a stereo-microscope (Olympus SZX16) for HR events identified as blue-stained cells or areas. The means of the three replicates are depicted. Statistical significance was tested with Mann-Whitney U-test in Minitab ([www.minitab.com](http://www.minitab.com)).

## Fresh weight measurements

Plants were grown as described in homologous recombination assays were measured on an analytical scale. Measuring was done in triplicates, and each sample was composed of 60 seedlings. Mann-Whitney U-test ( $P < 0.05$ ) was used to assess the significance of weight differences ([www.minitab.com](http://www.minitab.com)).

## RNA-seq data analysis

RNA-seq data for wild-type and *sog1-1* plants were obtained from a publicly available dataset (Bourbousse et al., 2018). The database contains gene expression values (fragment per kilobase per million reads, FPKM) in plants grown under normal and DNA damaging conditions at six-time points post gamma irradiation (20 min, 1.5, 3, 6, 12, and 24 h). From it, we acquired expression profiles of BCPs. The changes in gene expression were assessed as described in the results. For the assessment of statistical significance, we used a two-sample T-test with unequal variances.

## Reverse transcription-quantitative polymerase chain reaction

T-DNA mutants lines' seeds, sterilized and stratified, were grown on ½ MS medium with 0.6% agarose. Seven days old

seedlings were sampled and flash-frozen in liquid nitrogen. RNA extraction was performed by RNeasy Mini Kit (Qiagen, Cat. no. 74104). cDNA was constructed with RevertAid H Minus First Strand cDNA Synthesis Kit (Thermo Scientific™, Cat. no. K1631). The qPCR was performed with the HOT FIREPol® EvaGreen® qPCR Mix Plus (Solis BioDyne, Cat. no. 08-24-0000S) in CFX96 Touch Real-Time PCR Detection System. Wild type and *sog1-1* plants were grown for seven days in ½ MS 0.6% agarose and then transferred to liquid ½ MS with or without 40 µM MMC for a 1 h treatment. Following the treatment samples were flash-frozen in liquid nitrogen, and RNA extraction, cDNA synthesis and RT-qPCR were performed as described above. Mann-Whitney U-test was performed in Minitab to assess statistical significance of the data.

## Accession numbers

Gene information and sequences used in this article can be found in TAIR under the following accession numbers: *BCP1* (AT4G02110), *BCP2* (AT2G41450), *BCP3* (AT4G03130), *BCP4* (AT3G21480), *SMC6B* (AT5G61460).

## Results

### Identification of Arabidopsis BRCT5 domain-containing proteins

To identify potential Arabidopsis BRCT5 domain-containing proteins, we performed a BLAST search (Altschul et al., 1990) using the BRCT5 domains of the fission yeast *Schizosaccharomyces pombe* Brc1 (*SpBrc1*) and human *Homo sapiens* NSE5 (*HsNSE5*) proteins against the Arabidopsis protein database. Three candidates, At4g02110, At4g03130, and At4g21070, were found as potential genes of interest. We hypothesized that the large phylogenetic distance between Arabidopsis versus yeast and human might have reduced the efficiency of such a screen and compromised the direct identification of some candidates. Therefore, we performed an additional search for the BRCT5 domain-containing proteins in the genome of moss *Physcomitrium patens* using the same query sequences from *SpBrc1* and *HsNSE5*. The BRCT5 domains were found in the moss proteins Pp3c4\_1630, Pp3c7\_24750, Pp3c8\_2040, and Pp3c11\_4990. As the next step, the moss proteins were BLASTed against the Arabidopsis genome, which revealed three additional genes At1g04020, At2g41450, and At3g21480. The sequence comparison identified a conserved pattern of amino acids (Figure 1A) with different properties typical for the BRCT5 type domain that supported all the candidates identified *via* BLAST. The candidates At4g21070 and At1g04020 were previously described as *Arabidopsis* orthologs of human *BREAST CANCER SUSCEPTIBILITY 1* (*BRCA1*) and its homolog *BREAST CANCER ASSOCIATED RING 1* (*BARD1*), whose functions in plant DNA damage repair have been already

documented (Lafarge and Montané, 2003; Reidt et al., 2006). Therefore, both *BRCA1* and *BARD1* were excluded from subsequent analyses. Based on this, we selected the remaining four candidate proteins for further analysis and named them BRCT5 DOMAIN-CONTAINING PROTEINS (BCPs): BCP1 (At4g02110), BCP2 (At2g41450), BCP3 (At4g03130) and BCP4 (At3g21480). The superimposition of computationally modeled BRCT5 domains of *SpBrc1* and the four selected BCPs revealed their high structural similarity (Figure 1B). Based on Araport11 gene annotation, *BCP1* is a cell cycle regulated transcriptional coactivator (Menges et al., 2002). Based on its two BRCT domains, it was also considered a possible candidate for plant homolog of the human DNA topoisomerase 2-binding protein 1 (TOPBP1), but the overall low sequence similarity did not allow for the drawing of a firm conclusion (Shultz et al., 2007). *BCP2* is described as N-acetyltransferase (Araport11) and is expressed in the female gametophyte (Wuest et al., 2010). *BCP3* and *BCP4* are both described as BRCT domain-containing DNA repair proteins (Araport11), likely based on the presence of their C-terminal BRCT domains, with no further information. Hence, we

identified six BRCT5 domain-containing candidates in Arabidopsis, with four of them representing uncharacterized Arabidopsis genes.

### Loss of *BCP1* causes sensitivity to DNA damage, and its transcription is SOG1 dependent

To test for the potential role of BCPs in DNA damage repair, we isolated their T-DNA insertional mutants (Figure 2A). All homozygous mutants were viable and did not show any obvious developmental defects during somatic development and/or sterility during the reproductive stage.

As the first step, we performed an initial screening for mutant sensitivity to different types of DNA damage. The aim was to identify if any of the genes are important for DNA damage repair. To this end, we focused on the induction of all possible types of DNA damage including DSBs, DNA inter-strand, and DNA-protein crosslinks. Seeds were germinated, plants were grown on

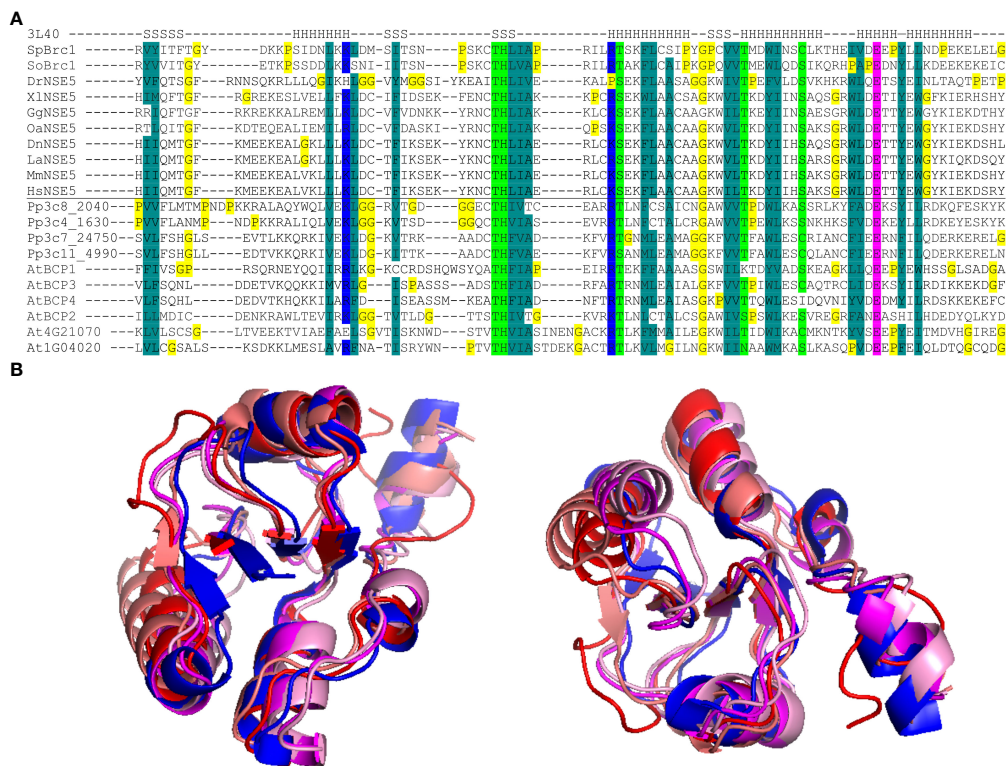


**FIGURE 1**  
BRCT5 domain analysis. (A) Alignment of the core part of the BRCT5 domain with helical (H) and  $\beta$ -strand (S) segments above (from PDB: 3L40 structure; Williams et al., 2010). The Brc1 and NSE5 orthologs are from *Schizosaccharomyces pombe* (Sp), *S. octosporus* (So), *Physcomitrium patens* (Pp), *Arabidopsis thaliana* (At), *Danio rerio* (Dr), *Xenopus laevis* (Xl), *Gallus gallus* (Gg), *Ornithorhynchus anatinus* (Oa), *Monodelphis domestica* (Md), *Dasyurus novemcinctus* (Dn), *Loxodonta africana* (La), *Mus musculus* (Mm), *Homo sapiens* (Hs). Coloring indicates amino acid groups conserved across the family: dark green, hydrophobic and aromatic; light green, polar; blue, acidic; pink, basic; all glycine and proline residues are highlighted in yellow. (B) Superimposition of modeled BRCT5 domains of At4g02110 (red), At2g41450 (deep pink), At4g03130 (pale pink), and crystal structure *SpBrc1* (blue) shown from two views.

the genotoxin-containing media, and their root length was measured (Figure 2B). The *smc6b-1* mutant allele of *STRUCTURAL MAINTENANCE OF CHROMOSOMES 6B* (*SMC6B*) served as a hypersensitive control. Under mock conditions, only the *bcp4-1* mutant plants had significantly shorter roots ( $9.4 \text{ mm} \pm 1.5 \text{ mm}$  in *bcp4-1* compared to  $13.23 \text{ mm} \pm 0.68 \text{ mm}$  in WT control), while the root length of the remaining mutants was not significantly different from the wild type (Figure 2C). Under DNA damaging conditions, the *bcp1-1* plants were hypersensitive to  $10 \mu\text{M}$  DNA inter-strand cross-linker MMC,  $20 \text{ nM}$  DNA-protein cross-linker CPT and  $20 \text{ nM}$  radiomimetic agent bleomycin causing DNA strand breaks. The *bcp1-1* plants also exhibited sensitivity to  $20 \mu\text{M}$  type I DNA-protein cross-linker zebularine (Prochazkova et al., 2022). The *bcp2-1*, *bcp3-1*, and *bcp4-1* mutant plants did not show significantly increased sensitivity to any of the genotoxic treatments (Figure 2D).

Absence of sensitivity in combination with non-coding sequence location of T-DNAs stimulated us to analyze the expression of BCPs in their corresponding T-DNA insertion mutant lines by RT-qPCR (Supplementary Figure 1). The *bcp1-1* and *bcp4-1* showed a very strongly reduced amount of transcript compared to their WT variants. Surprisingly, the *bcp2-1* with T-DNA insertion in the first out of total 13 exons showed more than 90-fold over-expression of *BCP2*. This might be caused by the expression from the *Cauliflower Mosaic Virus* 35S promoter that is part of the T-DNA insertion. The *bcp3-1* showed no significant difference in the amount of transcript compared to wild type. This suggests that *bcp1-1* and *bcp4-1* are loss of function mutants, *bcp2-1* is a potential overexpressor line and *bcp3-1* might not affect BCP3 gene function.

Next, we analyzed the expression of the BCP candidates using available transcriptomic data. Surprisingly, none of the selected candidates is represented on the Arabidopsis ATH1 expression array. RNA-sequencing-based atlas of Arabidopsis developmental stages (Klepikova et al., 2016) revealed that *BCP2* and *BCP3* were only weakly expressed throughout the whole plant development and that the expression slightly increased only in some floral parts (Supplementary Figure 2). In contrast, both *BCP1* and *BCP4* showed a low to moderate expression with the highest values observed in floral organs and seeds. Surprisingly, only weak expression was found in the root tissues. To find a potential involvement of BCPs in DNA damage response, we analyzed their expression after gamma-irradiation in wild-type and *sog1* mutant background using a publicly available RNA-seq dataset (Bourbousse et al., 2018). Under ambient (mock) conditions, *BCP1* was expressed stably at a basal level in both WT and *sog1-1* plants (Supplementary Figure 3A). In response to gamma-irradiation, *BCP1* was upregulated 3.2-fold already 20 min post-treatment, and the amount of transcript reached its 14-fold increase maximum 1.5 h post-irradiation (Figure 3A). The amount of transcript lowered over time and returned to mock levels 24 h after the treatment. In the *sog1* plants, gamma radiation-induced expression was not observed, suggesting that transcriptional response of *BCP1* to DNA damage is SOG1-dependent, and that *BCP1* acts

downstream of SOG1. This was confirmed also in RT-qPCR experiment where *BCP1* was significantly up-regulated in response to MMC treatment in wild-type but not in *sog1-1* mutant plants (Figure 3B). However, the same amount of *BCP1* expression in mock-treated wild-type and *sog1-1* plants indicates that basal *BCP1* expression is SOG1 independent. The remaining genes *BCP2*, *BCP3*, and *BCP4* showed only minor transcriptional changes that differed between wild-type and mutant plants, mostly at solitary time-points, suggesting that these genes are not gamma-irradiation inducible and their expression is not SOG1-dependent (Figure 3A).

To gain more insights into the transcriptional response of *BCP1* to DNA damage, we generated stable Arabidopsis transformants carrying *BCP1* promoter fused with the *GUS* reporter gene (*ProBCP1::GUS*). Under mock conditions, the *BCP1* promoter was active in tissues with actively dividing cells, such as the root and shoot apical meristems, lateral root meristems, and vasculature (Figure 3C<sub>2,3,4</sub>). The signals in true leaves had a peculiar dotted pattern. After inspection at the cellular level, it was obvious that these “dots” are represented by young stomata guard cells, stomatal lineage ground cells, and guard mother cells. The older (larger) stomata guard cells and pavement cells showed little or no *GUS* signals (Figure 3C<sub>5,6</sub>). As the Arabidopsis transcriptomic atlas (Klepikova et al., 2016) data suggested the highest *BCP1* transcript amount in reproduction (Supplementary Figure 2), we further examined the pattern of *BCP1* expression in inflorescences (Supplementary Figures 4A–E). We found particularly strong *GUS* signals in pistils throughout the entire flower development, young stamen, filaments, and perianth of closed flowers.

To visually confirm that the *BPC1* transcription is induced by DNA damage, as suggested by the transcriptomic data, we exposed seedlings of the *ProBCP1::GUS* reporter line to  $10 \mu\text{M}$  MMC for 24 h and subsequently scored *BCP1* promoter activity. Intense signals appeared in almost all parts of the plant, including the true leaves (Figure 3C<sub>7-12</sub>). This strongly supports transcriptomic data and demonstrates that *BCP1* transcription is inducible by DNA damage. Based on these experiments, we considered *BCP1* as the most promising candidate for further analysis.

## ***BCP1* is required for the repair of various types of DNA damage**

To validate our initial findings based on a single mutant allele, we isolated two more *BCP1* T-DNA-insertional mutants located in the 8<sup>th</sup> exon (*bcp1-2*) and the 7<sup>th</sup> intron (*bcp1-3*) (Figure 4A). Phenotypic analysis of all three homozygous mutant lines confirmed the absence of obvious developmental defects at four and six weeks of age (Supplementary Figure 5).

Next, we extended the sensitivity assays by exposing plants of all *bcp1* mutant lines to  $10 \mu\text{M}$  MMC,  $20 \mu\text{M}$  zebularine, and

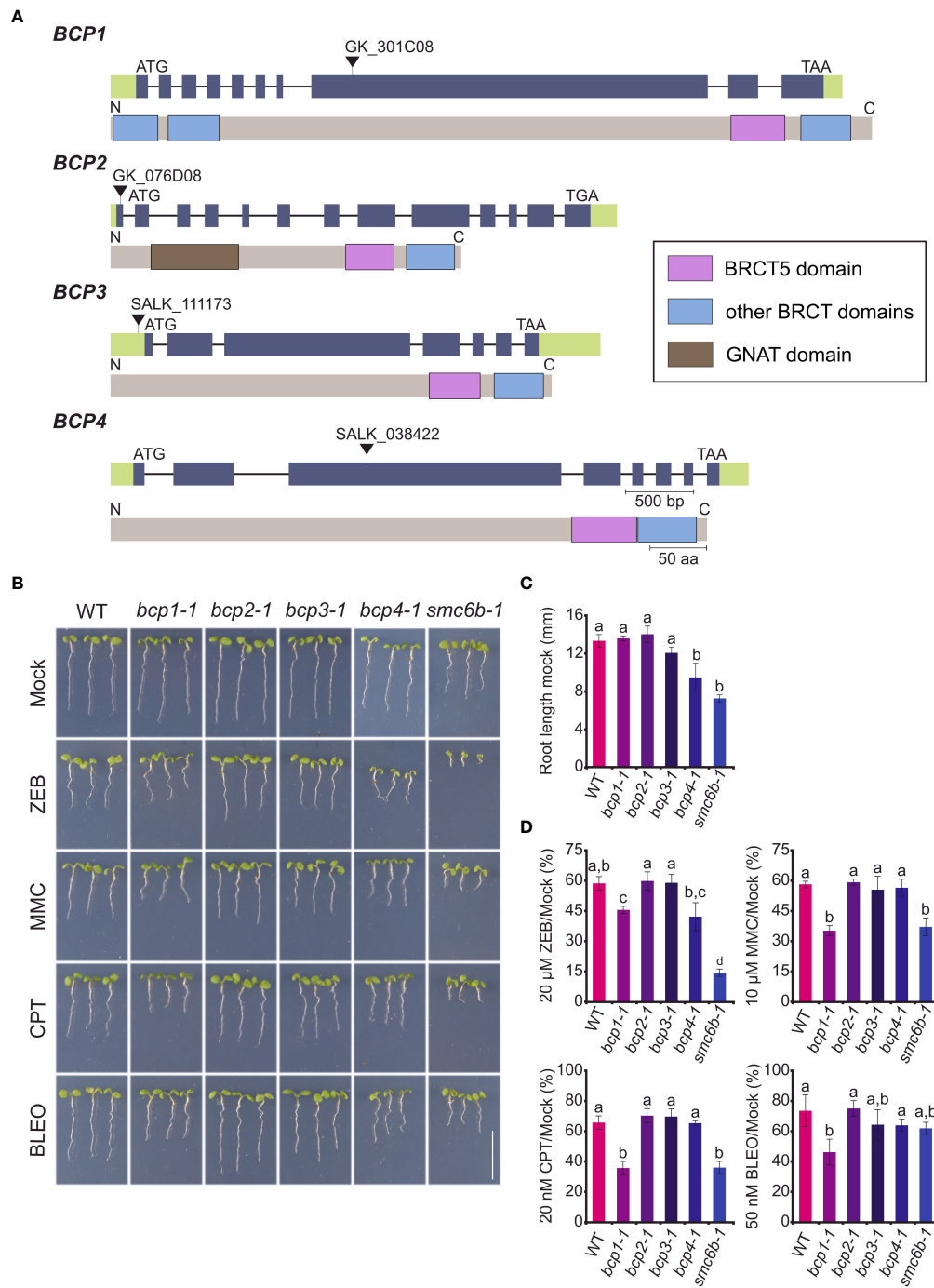


FIGURE 2

Phenotypes of mutants in uncharacterized Arabidopsis BRCT5 domain-containing genes. (A) Gene and protein structures of the BRCT5 CONTAINING PROTEINS (BCPs). The positions of T-DNAs in the used mutant alleles are indicated by black triangles above the gene models. Introns are indicated by a horizontal line and exons by green (untranslated regions) and purple (coding sequence) colors. Protein models under gene models (grey) show the position of known domains: BRCT - blue rectangles and GNAT (Gcn5-related N-acetyltransferase) - brown rectangle. (B) Representative phenotypes of seven days old wild-type (WT) and homozygous mutant plants grown on media containing 20  $\mu$ M zebularine (ZEB), 10  $\mu$ M mitomycin C (MMC), 20 nM camptothecin (CPT), 50 nM bleocin (BLEO). The *smc6b-1* served as a sensitive control. Scale bar = 1 cm. (C) Root length of WT and mutant plants under control (mock) conditions. Error bars indicate the standard deviation between the means of three biological replicates. The letters above columns indicate similarities between samples. The same letters indicate samples that were not significantly different in one-way ANOVA with *post hoc* Tukey's test ( $P < 0.05$ ). (D) Root length of WT and mutants from B under DNA damaging treatments relative to the growth of the same genotype under mock conditions. Error bars represent the standard deviation between three biological replicates, each with at least 15 plants. Statistics were performed as in (C).

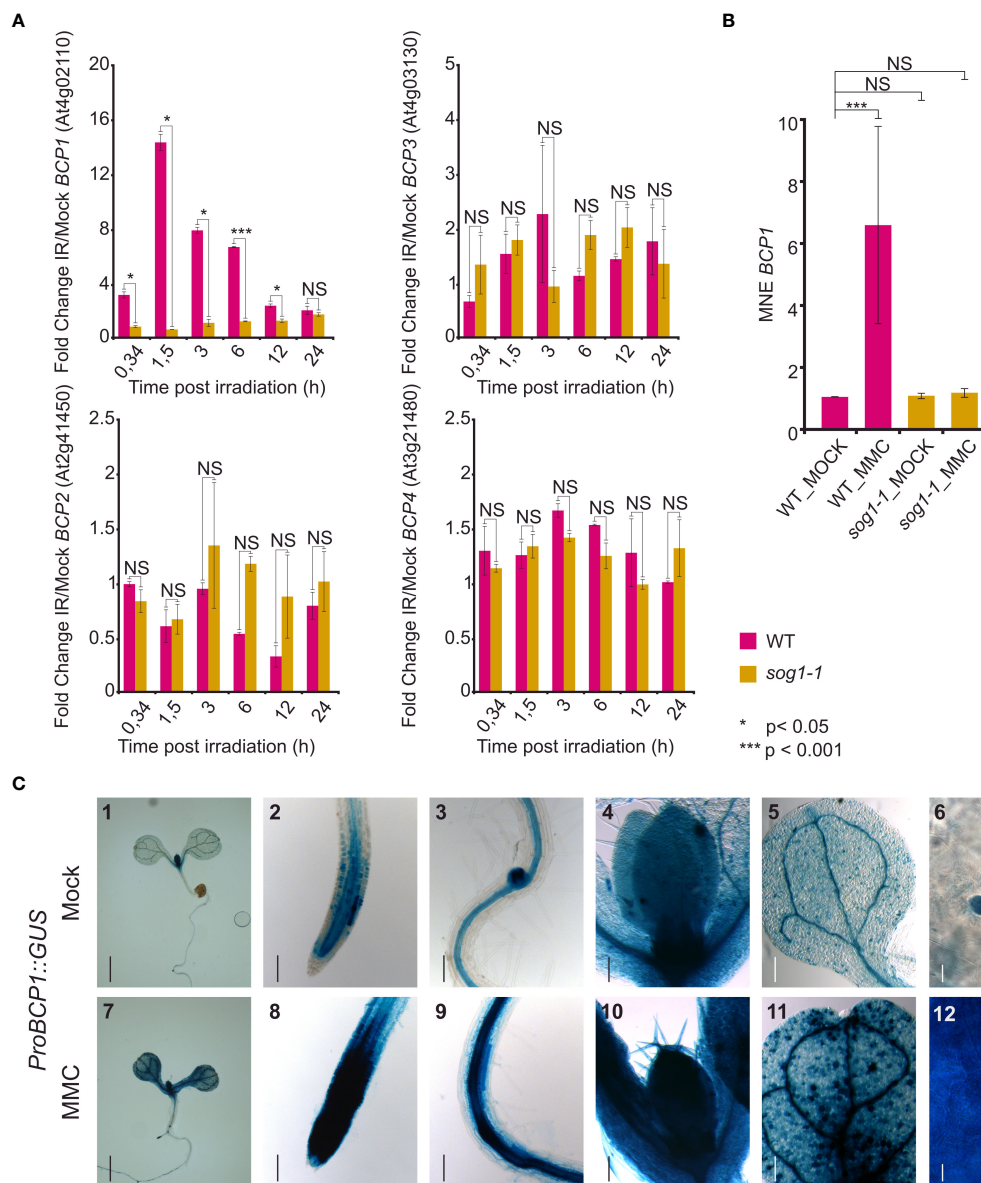


FIGURE 3

Expression of the *BCP* genes. **(A)** Relative expression of *BCP1* to *BCP4* in wild type (WT) and *sog1-1* based on RNA-sequencing experiment of Bourbousse et al. (2018). The normalized read counts from RNA-sequencing (FPKM) were used to calculate fold change in expression after gamma irradiation pulse (IR) versus mock conditions (y-axis). The x-axis indicates the harvesting time after the irradiation treatment. Error bars represent the standard error of the mean. Asterisks represent significant differences in two sample T-test with unequal variance, \*  $P < 0.05$ , \*\*\*  $P < 0.001$ , NS – not significantly different. **(B)** Reverse transcription qPCR analysis of *BCP1* expression in wild-type (WT) and *sog1-1* plants without (MOCK) and after 1 h treatment with 40  $\mu$ M MMC (MMC). Y-axis shows mean normalized expression relative to *PP2A*. Error bars show three biological replicates. NS = not significantly different, \*\*\* statistically significantly different in Mann-Whitney U-test at  $P < 0.05$ . **(C)** *In planta* analysis of *BCP1* promoter activity. Seven days old seedlings carrying *ProBCP1::GUS* were transferred to mock and DNA damaging conditions for 24h. *BCP1* promoter activity was monitored using GUS histochemical staining. Representative stereo microscope pictures of tissues showing the gene expression. (1,7) Whole seedling, (2, 8) shoot apical meristem, (3, 9) lateral root meristem, (4, 10) shoot apical meristem with first real leaves, (5, 11) cotyledon, (6, 12) leaf blade cells. Scale bars: 1,7 = 1 mm; 2-5,8-11 = 100  $\mu$ m, 6,12 = 50  $\mu$ m.

20 nM CPT (Figures 4B, D). In mock conditions *bcp1-1* and *bcp1-2* mutants showed no difference in root length compared to wild type, while *bcp1-3* plants had slightly longer roots (Figure 4C). Both *bcp1-1* and *bcp1-2* alleles were significantly

sensitive to all three drug treatments. In contrast, the intronic mutant *bcp1-3* was hypersensitive only to 10  $\mu$ M MMC (Figure 4D). This is in agreement with the amount of *BCP1* transcript which was almost not detectable in *bcp1-1* and *bcp1-2*

mutants but was not significantly reduced in *bcp3-1* (Supplementary Figure 1). Specifically, MMC-treated wild-type plants reached  $38.8 \pm 3.6\%$  of the standard root length compared to mock conditions, while it was only  $21.8 \pm 1.7\%$ ,  $25.5 \pm 2.5\%$ , and  $27 \pm 3\%$  of the mock-treated plant root length for *bcp1-1*, *bcp1-2*, and *bcp1-3*, respectively (all comparisons  $P < 0.001$  one-way ANOVA with *post hoc* Tukey HSD). Zebularine-treated wild-type plants reached  $53.3 \pm 1.7\%$  of the mock control length. For zebularine treated *bcp1-1*, *bcp1-2* and *bcp1-3* plants it was  $42.7 \pm 5.6\%$ ,  $41.6 \pm 1.25\%$  and  $50.5 \pm 4.0\%$ , respectively (all comparisons  $P < 0.001$ ). Similarly, CPT-treated wild-type plants reached  $43.2 \pm 4\%$  of the normal root length, but it was  $25.5 \pm 1.1\%$ ,  $37.4 \pm 1.4\%$ , and  $47.5 \pm 2\%$  for the individual *bcp1* mutant alleles, respectively (all comparisons  $P < 0.001$  one-way ANOVA with *post hoc* Tukey HSD). The sensitive control *smc6b-1* plants had massive root length reduction to  $16 \pm 2\%$ ,  $10 \pm 0.3\%$ , and  $20 \pm 1\%$  for MMC, zebularine, and CPT (all comparisons  $P < 0.001$  one-way ANOVA with *post hoc* Tukey HSD).

To assess the extent of damage at the cellular level, we performed a cell death assay based on the staining of root apices with propidium iodide (PI), where PI marks the dead cells and is excluded from the living cells (Figures 4E, F). Wild-type and *smc6b-1* were used as standard and hypersensitive controls. Mock-treated wild-type and *bcp1* plants showed no significantly different mean values of less than one dead cell per root (Figures 4E, F). After the treatment with  $10 \mu\text{M}$  MMC for 24 h, the median number of dead cells per root increased to three in wild type, four in *bcp1-2* and *bcp1-3*, and five in *bcp1-1* (Figure 4F). The values in all mutant lines were significantly higher compared to wild-type plants. This shows that loss of function from *BCP1* makes Arabidopsis plants hypersensitive to diverse types of DNA damage and leads to increased cell death.

## BCP1 is required for normal frequency of homologous recombination

Based on the SOG1-dependent transcriptional activation of *BCP1* upon DNA damage and hypersensitivity of *bcp1* plants to DNA damaging treatments, we hypothesized about a possible role of *BCP1* in HR. To experimentally test this hypothesis, we generated double homozygous *bcp1-1 B11* and *bcp1-1 IC9C* lines (Swoboda et al., 1994; Puchta et al., 1995; Molinier et al., 2004). Owing to the organization of the reporter regions, these lines allow locus-specific monitoring of the frequency of single-strand annealing (SSA) and synthesis-dependent strand annealing (SDSA) types of HR, respectively (Orel et al., 2003). The plants were germinated and grown on media without (mock) and with  $1 \mu\text{M}$  MMC for 10 days and analyzed for HR events. There were no significant differences (Mann-Whitney U test,  $P > 0.05$ ) in fresh weight between all genotypes (Supplementary Figure 6), indicating similar number of cells. Under mock conditions, we found on average  $2.9 \pm 2.2$  SSA HR events per

*B11* wild type ( $n = 131$ ) plant (Figure 5), while *bcp1-1 B11* plants ( $n = 151$ ) showed 52% less SSA HR events per plant ( $1.4 \pm 1.5$ ). This difference was statistically significantly different ( $P < 0.001$  Mann-Whitney U-test), indicating a possible role of *BCP1* in HR independent of exogenous DNA damage. In response to a mild DNA inter-strand crosslinking treatment by MMC, there were on average  $34 \pm 12$  SSA HR events per *B11* plant ( $n = 137$  plants) and  $21 \pm 10.6$  per *bcp1-1 B11* plant ( $n = 151$  plants), corresponding to a significant ( $P < 0.001$  Mann-Whitney U-test) 38% reduction in the mutant.

A similar pattern was observed in SDSA HR reporter line IC9C. Also here, we did not find significant differences (Mann-Whitney U-test,  $P > 0.05$ ) in fresh weight between all genotypes (Supplementary Figure 6), indicating similar number of cells. The IC9C wild type and IC9C *bcp1-1* lines showed a similar  $0.2 \pm 0.46$  ( $n = 153$  plants) and  $0.28 \pm 0.61$  ( $n = 109$  plants) SDSA events per plant under mock conditions, respectively. After treatment with  $1 \mu\text{M}$  MMC, IC9C wild type showed an average of  $1.59 \pm 1.31$  ( $n = 102$  plants) SDSA HR events plant, while IC9C *bcp1-1* line had  $0.78 \pm 0.85$  ( $n = 158$  plants) SDSA HR events per plant. This is a 50.5% decrease in the number of HR events in the *bcp1-1* mutant under mild genotoxic stress. Collectively, this shows that *BCP1* is needed for normal levels of SSA and SDSA HR in Arabidopsis and suggests an involvement of *BCP1* in the HR repair.

## Discussion

In this work, we found a new Arabidopsis protein *BCP1* which contains the BRCT5 domain and contributes to DNA damage repair by homologous recombination in a SOG1-dependent manner.

To identify Arabidopsis BRCT5 domain-containing proteins, we performed a homology search using fission yeast *SpBrc1* and human *HsNSE5*. These proteins were selected because they are known to mediate interactions of the conserved SMC5/6 DNA repair complex to chromatin (Li et al., 2012; Räschle et al., 2015). While human *NSE5* directly contains the BRCT5 domain, the yeast *NSE5* does not, but it binds BRCT5-containing *Brc1* protein which targets it to DNA damage sites. The situation in Arabidopsis resembles yeast where none of the currently known SMC5/6 complex subunits harbors a BRCT domain (Yan et al., 2013). Hence, identification of the plant BRCT5 domain-containing proteins might lead to a plant-specific SMC5/6 cofactor mediating interaction with DNA repair complexes and/or chromatin.

Via two BLASTs, first against the moss *Physcomitrium patens* and then Arabidopsis, we found in total six Arabidopsis BRCT5 domain-containing proteins, including two already known DNA damage repair factors *BRCA1* and *BARD1*. *BRCA1* is a well-known tumor suppressor in humans that is evolutionarily conserved also in plants (Trapp et al., 2011). Studies in

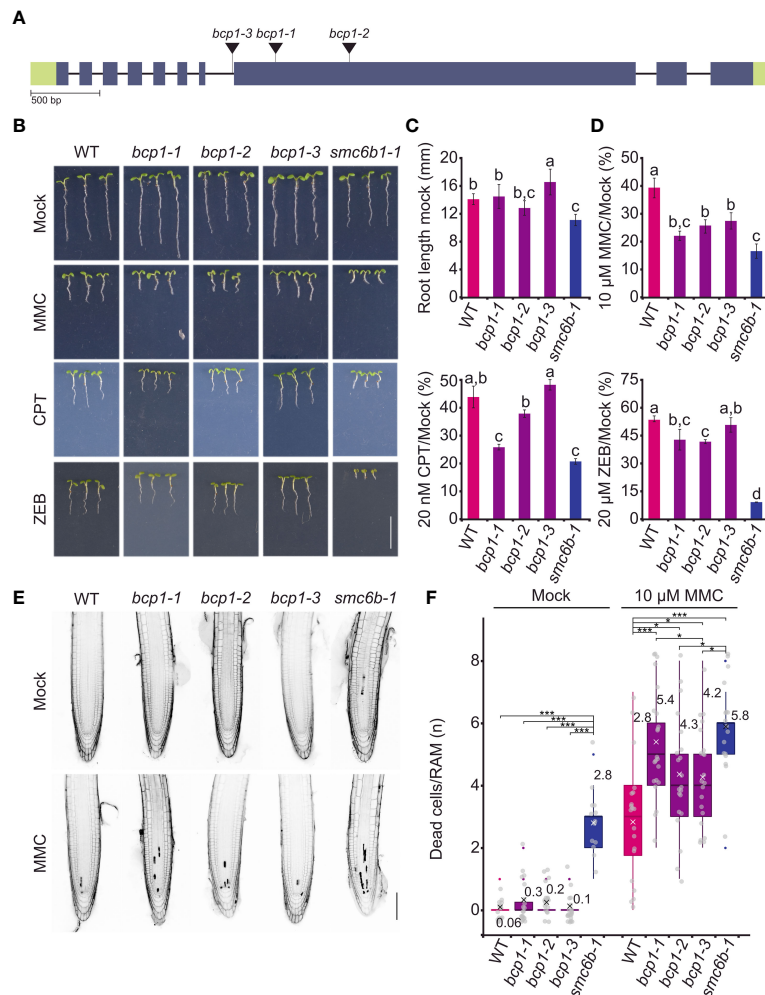


FIGURE 4

BCP1 is required for normal resistance to DNA damaging treatments. **(A)** Gene model of BCP1 with indicated positions of all used T-DNA insertional mutants. The style follows the description in Figure 2A. **(B)** DNA damage sensitivity assays of different *bcp1* alleles. Representative phenotypes of seven days old wild-type (WT) and homozygous mutant plants grown on media containing 20 μM zebularine (ZEB), 10 μM mitomycin C (MMC), and 20 nM camptothecin (CPT). The *smc6b-1* served as a sensitive control. Scale bar = 1 cm. **(C)** Root length of WT and mutant plants grown under control (mock) conditions. Error bars indicate the standard deviation between the means of nine biological replicates. The letters above columns indicate similarity between samples. The same letters indicate samples that were not significantly different in one-way ANOVA with posthoc Tukey's test ( $P < 0.05$ ). **(D)** Root length of WT and mutants under DNA damaging treatments relative to the growth of the same genotypes under mock conditions. Statistics were performed as in **(C)**. **(E)** Representative confocal microscopy images of the primary roots stained by propidium iodide in cell death assays. Five days old seedlings of WT and *bcp1* mutants were exposed to mock or 10 μM MMC treatments for 24 h, stained with propidium iodide, and analyzed to reveal dead cells that appear as dark sectors inside the roots. The *smc6b-1* served as a control with increased cell death. Scale bar = 100 μm. **(F)** Quantification of dead cells per root apical meristem in different genotypes and treatments (complements E). Each gray dot indicates the number of dead cells per root ( $n = 13-22$ ). The boxplots' hinges are in the 1st and 3rd quartile, with a marked median. The mean is indicated by a cross with a numerical value. Whisker marks show the lowest or highest value within the 1.5 interquartile range below or above hinges. Statistical significance was tested by Kruskal-Wallis H-test with post hoc Conover-Iman test of multiple comparisons with Benjamini-Hochberg procedure ( $P < 1/2 \alpha$ ,  $\alpha = 0.05$ ). NS - not significant, \*  $P < 0.025$ , \*\*\*  $P < 0.001$ .

mammals and Arabidopsis revealed that BRCA1 and BARD1 frequently act as a heterodimer (Wu et al., 1996; Reidt et al., 2006). In Arabidopsis, both BRCA1 and BARD1 are necessary for resistance to DNA damage and also for normal levels of somatic homologous recombination (Reidt et al., 2006). Furthermore, the function of BARD1 seems to go beyond the regulation of genome

stability because BARD1 was found to suppress the expression of *WUSCHEL1*, a master regulator homeobox gene controlling the stem cell pool (Mayer et al., 1998), in the shoot apical meristems and thus contributing to the meristem normal growth and organization during plant development (Han et al., 2008). Besides the established role of these two proteins in plant DNA

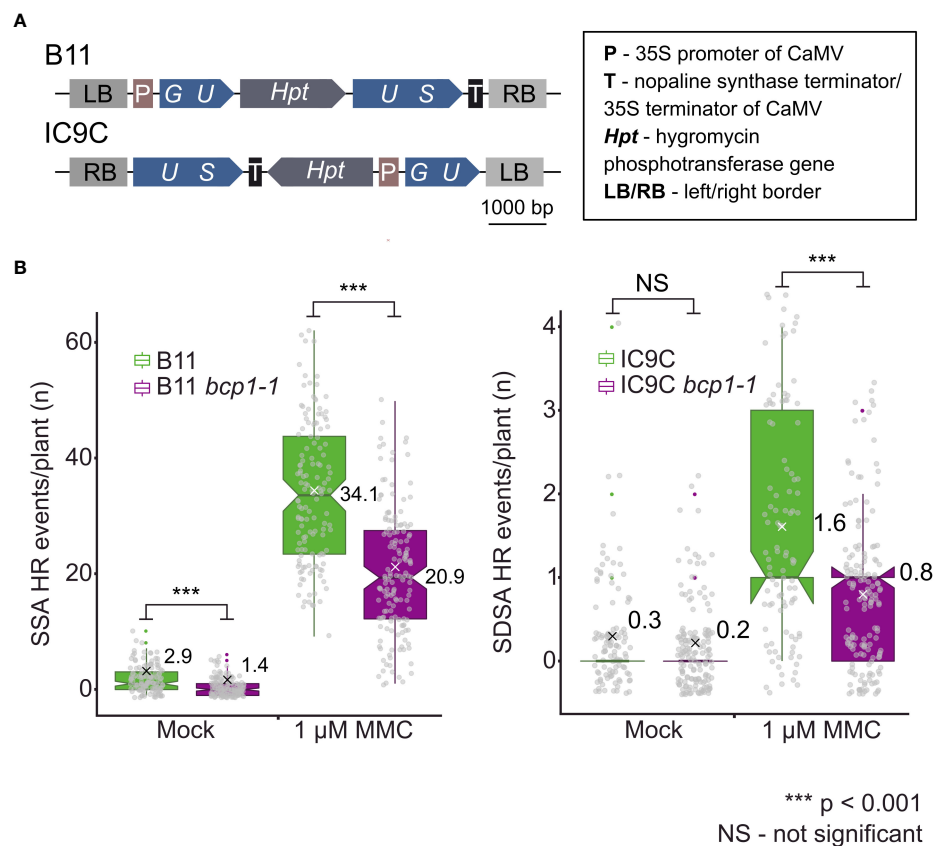


FIGURE 5

(A) Schematic model of constructs used to create *B11* and *IC9C* HR reporter lines (Swoboda et al., 1994; Molinier et al., 2004). (B) Loss of BCP1 causes reduced frequency of somatic homologous recombination (HR). Wild type (WT) and *bcp1-1* plants carrying genomic substrates for single-strand annealing (*B11*) and synthesis-dependent strand annealing (*IC9C*) types of HR were grown on mock and 1 µM containing MMC media for 10 days. Gray dots indicate HR events per plant. The boxplots' hinges are in the 1<sup>st</sup> and 3<sup>rd</sup> quartile, with a marked median. Mean is represented by a cross with a numerical value. Whisker marks show the lowest or highest value within the 1.5 interquartile range below or above hinges. Asterisks represent significant differences in Mann-Whitney U-test \*\*\*  $P < 0.001$ , NS – not significantly different.

damage repair, their exact molecular functions, including the binding targets of BRCT5 domains, remain unknown.

The BCP2, BCP3, and BCP4 proteins carry a pair of BRCT domains only at their C-termini. On contrary, BCP1 bears an additional pair of BRCT domains also at the N-terminus. The BRCT5 domain of all Arabidopsis BCPs shows a conserved pattern of specific amino acids with different properties. Furthermore, *in silico*-based modeling revealed a conserved structure of this domain in plants relative to the fission yeast Brc1. The only non-BRCT domain identified in BCPs was an N-terminally positioned Gcn5-related N-acetyltransferase domain (Uniprot) in BCP2. It implies that BCP2 might contribute to chromatin relaxation and/or transcription. However, none of the BCPs repeated the repertoire of domains in *SpBrc1* and/or *HsNSE5*, suggesting that they are not direct Arabidopsis homologs, and biochemical studies will have to be conducted to explore their potential relationship at the protein-protein interaction level. BCP1 shows possible homologies to the human

proteins PTIP and TOPI1B. However, a significant homology is present only over the BRCT domain regions. Based on this, we conclude that all four identified BCPs represent novel plant-specific BRCT5 domain-containing proteins.

An important step toward the functional characterization of the BCPs was their response to DNA damage. The most promising candidate in DNA damage sensitivity assays was *BCP1*, while *BCP2*, *BCP3*, and *BCP4* did not differ significantly from wild-type. However, analysis of additional mutant alleles for at least *BCP2* and *BCP3* is needed because the alleles tested in this study most likely do not represent loss of function mutants. The *bcp2-1* allele may even be a *BCP2* overexpressor line. BCP1 loss-of-function mutants were hypersensitive to DNA DSBs caused by bleocin, DNA-inter-strand crosslinks induced by MMC, and two types of DNA-protein crosslinks caused by zebularine and CPT. Hence, BCP1 emerged from our analyses as an important player in DNA repair of multiple types of DNA lesions, possibly through a mainstream DNA repair pathway. The possible role of BCP2,

BCP3, and BCP4 in e.g. repair of other types of DNA damage is not excluded and should be a focus of future studies.

We made an exciting observation that BCP1 is transcriptionally upregulated in response to gamma-radiation and MMC treatments and that the activation is SOG1-dependent. SOG1 is a plant-specific transcription factor that is phosphorylated by ATM and ATR kinases and orchestrates downstream responses of the key set of genes involved in the maintenance of genome stability, including cell cycle and homologous recombination repair (Yoshiyama et al., 2013a; Yoshiyama, 2016; Ogita et al., 2018). Two recent studies defined the SOG1 consensus binding motif CTT(N)<sub>7</sub>AAG and found that SOG1 is physically binding to the cis-regulatory region of *BCP1* in Arabidopsis (Bourbousse et al., 2018; Ogita et al., 2018). Surprisingly, we did not find any such a motif in the region upstream of the *BCP1* transcription start site which suggests a presence of a non-canonical SOG1 binding motif in the *BCP1* promoter.

The absence of *BCP1* transcriptional upregulation in the *sog1* mutant background also clearly places *BCP1* downstream of SOG1 in the same DNA damage repair pathway. Although *BCP1* transcription is enhanced by DNA damage, it is not fully dependent on it. This is apparent from the expression of *BCP1* promoter in both somatic and floral meristems without any stress. Our analysis suggests that *BCP1* is activated to a basal level in SOG1-independent and induced-DNA damage-independent manner. Whether this represents an activation induced by spontaneously occurring DNA damage (e.g. during DNA replication) remains to be studied. In summary, we identify *BCP1* as an Arabidopsis BRCT5 domain-containing gene directly transcriptionally controlled by SOG1 during induced DNA damage.

The critical experiment was the analysis of somatic homologous recombination using genetically engineered HR trap lines. This experiment showed a significantly reduced frequency of HR in *bcp1* mutant plants, strongly suggesting that BCP1 is needed for normal levels of HR. How BCP1 directly functions in this process is currently unknown. By its N- and C-terminal BRCT domains, it could bind two phosphorylated proteins and this way facilitate HR. Such interactors will be identified in the follow-up research.

In conclusion, out of four uncharacterized Arabidopsis BRCT5 domain-containing proteins, we identified BCP1 as a new Arabidopsis DNA damage repair factor that is directly controlled by SOG1 and ensures normal levels of homologous recombination.

## Data availability statement

The datasets presented in this study can be found in online repositories. The names of the repository/repositories and accession number(s) can be found below: <https://www.ncbi.nlm.nih.gov/geo/>, GSE112773.

## Author contributions

AP, JP, JD, and JV conceived and designed the study. JV, FY, and ET performed experiments. All authors analyzed data and interpreted the results. AP and JV wrote the paper. All authors contributed to the article and approved the submitted version.

## Funding

This work was supported by a Purkyně Fellowship from the Czech Academy of Sciences and Czech Science Foundation project 22-00871S (all to AP), China Scholarship Council Fellowship (File No. 201604910685), and the Fisher Scholarship from the Palacký University in Olomouc (both to FY). JV, ET, and AP were additionally supported by the ERDF project “Plants as a tool for sustainable global development” (No. CZ.02.1.01/0.0/0.0/16\_019/0000827). JJP was funded by the Czech Science Foundation project GA20-05095S.

## Acknowledgments

We thank E. Jahnová, H. Tvardíková, and Z. Bursová for excellent technical assistance and Dr. Inna Lermontova for the donation of the *pKGWFS7.0* vector and Dr. Julie Law for the FPKM values from DNA damage RNA-seq experiment.

## Conflict of interest

The authors declare that the research was conducted in the absence of any commercial or financial relationships that could be construed as a potential conflict of interest.

## Publisher's note

All claims expressed in this article are solely those of the authors and do not necessarily represent those of their affiliated organizations, or those of the publisher, the editors and the reviewers. Any product that may be evaluated in this article, or claim that may be made by its manufacturer, is not guaranteed or endorsed by the publisher.

## Supplementary material

The Supplementary Material for this article can be found online at: <https://www.frontiersin.org/articles/10.3389/fpls.2022.1023358/full#supplementary-material>

## References

- Alonso, J. M., Stepanova, A. N., Leisse, T. J., Kim, C. J., Chen, H., Shinn, P., et al. (2003). Genome-wide insertional mutagenesis of arabidopsis thaliana. *Science* 301, 653–657. doi: 10.1126/science.1086391
- Altschul, S. F., Gish, W., Miller, W., Myers, E. W., and Lipman, D. J. (1990). Basic local alignment search tool. *J. Mol. Biol.* 215, 403–410. doi: 10.1016/S0022-2836(05)80360-2
- Baubec, T., Pecinka, A., Rozhon, W., and Mittelsten Scheid, O. (2009). Effective, homogeneous and transient interference with cytosine methylation in plant genomic DNA by zebularine. *Plant J.* 57, 542–554. doi: 10.1111/j.1365-313X.2008.03699.x
- Bork, P., Hofmann, K., Bucher, P., Neuwald, A. F., Altschul, S. F., and Koonin, E. V. (1997). A superfamily of conserved domains in DNA damage- responsive cell cycle checkpoint proteins. *FASEB J.* 11, 68–76. doi: 10.1096/fasebj.11.1.9034168
- Bourbousse, C., Vegesna, N., and Law, J. A. (2018). SOG1 activator and MYB3R repressors regulate a complex DNA damage network in arabidopsis. *Proc. Natl. Acad. Sci. U.S.A.* 115, E12453–E12462. doi: 10.1073/pnas.1810582115
- Chatterjee, N., and Walker, G. C. (2017). Mechanisms of DNA damage, repair, and mutagenesis. *Environ. Mol. Mutagen.* 58, 235–263. doi: 10.1002/em.22087
- Hafner, A., Bulyk, M. L., Jambhekar, A., and Lahav, G. (2019). The multiple mechanisms that regulate p53 activity and cell fate. *Nat. Rev. Mol. Cell Biol.* 20, 199–210. doi: 10.1038/s41580-019-0110-x
- Han, P., Li, Q., and Zhu, Y.-X. (2008). Mutation of arabidopsis BARD1 causes meristem defects by failing to confine WUSCHEL expression to the organizing center. *Plant Cell* 20, 1482–1493. doi: 10.1105/tpc.108.058867
- Heyer, W.-D., Ehmsen, K. T., and Liu, J. (2010). Regulation of homologous recombination in eukaryotes. *Annu. Rev. Genet.* 44, 113–139. doi: 10.1146/annurev-genet-051710-150955
- Hu, Z., Cools, T., and De Veylder, L. (2016). Mechanisms used by plants to cope with DNA damage. *Annu. Rev. Plant Biol.* 67, 439–462. doi: 10.1146/annurev-arplant-043015-111902
- Kleinboelting, N., Huep, G., Kloetgen, A., Viehoveer, P., and Weisshaar, B. (2012). GABI-kat SimpleSearch: new features of the arabidopsis thaliana T-DNA mutant database. *Nucleic Acids Res.* 40, D1211–D1215. doi: 10.1093/nar/gkr1047
- Klepikova, A. V., Kasianov, A. S., Gerasimov, E. S., Logacheva, M. D., and Penin, A. A. (2016). A high resolution map of the arabidopsis thaliana developmental transcriptome based on RNA-seq profiling. *Plant J.* 88, 1058–1070. doi: 10.1111/tj.13312
- Lafarge, S., and Montané, M.-H. (2003). Characterization of arabidopsis thaliana ortholog of the human breast cancer susceptibility gene 1: AtBRCA1, strongly induced by gamma rays. *Nucleic Acids Res.* 31, 1148–1155. doi: 10.1093/nar/gkg202
- Leung, G. P., Lee, L., Schmidt, T. I., Shirahige, K., and Kobor, M. S. (2011). Rtt107 is required for recruitment of the SMC5/6 complex to DNA double strand breaks. *J. Biol. Chem.* 286, 26250–26257. doi: 10.1074/jbc.M111.235200
- Li, X., Liu, K., Li, F., Wang, J., Huang, H., Wu, J., et al. (2012). Structure of c-terminal tandem BRCT repeats of Rtt107 protein reveals critical role in interaction with phosphorylated histone H2A during DNA damage repair. *J. Biol. Chem.* 287, 9137–9146. doi: 10.1074/jbc.M111.311860
- Lobet, G., Pagès, L., and Draye, X. (2011). A novel image-analysis toolbox enabling quantitative analysis of root system architecture. *Plant Physiol.* 157, 29–39. doi: 10.1104/pp.111.179895
- Manova, V., and Gruszka, D. (2015). DNA Damage and repair in plants – from models to crops. *Front. Plant Sci.* 6. doi: 10.3389/fpls.2015.00885
- Mayer, K. F. X., Schoof, H., Haecker, A., Lenhard, M., Jürgens, G., and Laux, T. (1998). Role of WUSCHEL in regulating stem cell fate in the arabidopsis shoot meristem. *Cell* 95, 805–815. doi: 10.1016/S0092-8674(00)81703-1
- Menges, M., Hennig, L., Gruissem, W., and Murray, J. A. H. (2002). Cell cycle-regulated gene expression in Arabidopsis \*. *J. Biol. Chem.* 277, 41987–42002. doi: 10.1074/jbc.M207570200
- Molinier, J., Ries, G., Bonhoeffer, S., and Hohn, B. (2004). Interchromatid and interhomolog recombination in arabidopsis thaliana. *Plant Cell* 16, 342–352. doi: 10.1105/tpc.019042
- Nisa, M.-U., Huang, Y., Benhamed, M., and Raynaud, C. (2019). The plant DNA damage response: signaling pathways leading to growth inhibition and putative role in response to stress conditions. *Front. Plant Sci.* 10. doi: 10.3389/fpls.2019.00653
- Ogita, N., Okushima, Y., Tokizawa, M., Yamamoto, Y. Y., Tanaka, M., Seki, M., et al. (2018). Identifying the target genes of SUPPRESSOR OF GAMMA RESPONSE 1, a master transcription factor controlling DNA damage response in arabidopsis. *Plant J.* 94, 439–453. doi: 10.1111/tj.13866
- Oravcová, M., Gadaleta, M. C., Nie, M., Reubens, M. C., Limbo, O., Russell, P., et al. (2019) BrC1 promotes the focal accumulation and SUMO ligase activity of Smc5-Smc6 during replication stress. In: *Molecular and cellular biology*. Available at: <https://journals.asm.org/doi/full/10.1128/MCB.00271-18> (Accessed May 11, 2022).
- Orel, N., Kyryk, A., and Puchta, H. (2003). Different pathways of homologous recombination are used for the repair of double-strand breaks within tandemly arranged sequences in the plant genome. *Plant J.* 35, 604–612. doi: 10.1046/j.1365-313X.2003.01832.x
- Preuss, S. B., and Britt, A. B. (2003). A DNA-damage-induced cell cycle checkpoint in arabidopsis. *Genetics* 164, 323–334. doi: 10.1093/genetics/164.1.323
- Prochazkova, K., Finke, A., Tomašiková, E. D., Filo, J., Bente, H., Dvořák, P., et al. (2022). Zebularine induces enzymatic DNA–protein crosslinks in 45S rDNA heterochromatin of arabidopsis nuclei. *Nucleic Acids Res.* 50, 244–258. doi: 10.1093/nar/gkab1218
- Puchta, H., Swoboda, P., and Hohn, B. (1995). Induction of intrachromosomal homologous recombination in whole plants. *Plant J.* 7, 203–210. doi: 10.1046/j.1365-313X.1995.7020203.x
- R Core Team. (2018). *R: A Language and Environment for Statistical Computing* (Vienna: R Foundation for Statistical Computing). Available at: <https://www.R-project.org>.
- Räschle, M., Smeenk, G., Hansen, R. K., Temu, T., Oka, Y., Hein, M. Y., et al. (2015). Proteomics reveals dynamic assembly of repair complexes during bypass of DNA cross-links. *Science* 348, 1253671. doi: 10.1126/science.1253671
- Razqallah, H. (2008). DNA-Damage repair; the good, the bad, and the ugly. *EMBO J.* 27, 589–605. doi: 10.1038/emboj.2008.15
- Reidt, W., Wurz, R., Wanieck, K., Ha Chu, H., and Puchta, H. (2006). A homologue of the breast cancer-associated gene BARD1 is involved in DNA repair in plants. *EMBO J.* 25, 4326–4337. doi: 10.1038/sj.emboj.7601313
- Seton-Rogers, S. (2006). Putting p53 in context. *Nat. Rev. Cancer* 6, 423–423. doi: 10.1038/nrc1924
- Shultz, R. W., Tatineni, V. M., Hanley-Bowdoin, L., and Thompson, W. F. (2007). Genome-wide analysis of the core DNA replication machinery in the higher plants arabidopsis and rice. *Plant Physiol.* 144, 1697–1714. doi: 10.1104/pp.107.101105
- Swoboda, P., Gal, S., Hohn, B., and Puchta, H. (1994). Intrachromosomal homologous recombination in whole plants. *EMBO J.* 13, 484–489. doi: 10.1002/j.1460-2075.1994.tb06283.x
- Trapp, O., Seeliger, K., and Puchta, H. (2011). Homologs of breast cancer genes in plants. *Front. Plant Sci.* 2. doi: 10.3389/fpls.2011.00019
- Varadi, M., Anyango, S., Deshpande, M., Nair, S., Natassia, C., Yordanova, G., et al. (2022). AlphaFold protein structure database: massively expanding the structural coverage of protein-sequence space with high-accuracy models. *Nucleic Acids Res.* 50, D439–D444. doi: 10.1093/nar/gkab1061
- Wan, B., Hang, L. E., and Zhao, X. (2016). Multi-BRCT scaffolds use distinct strategies to support genome maintenance. *Cell Cycle* 15, 2561–2570. doi: 10.1080/15384101.2016.1218102
- Williams, J. S., Williams, R. S., Dovey, C. L., Guenther, G., Tainer, J. A., and Russell, P. (2010). gammaH2A binds BrC1 to maintain genome integrity during s-phase. *EMBO J.* 29, 1136–1148. doi: 10.1038/emboj.2009.413
- Wuest, S. E., Vijverberg, K., Schmidt, A., Weiss, M., Gheyselinck, J., Lohr, M., et al. (2010). Arabidopsis female gametophyte gene expression map reveals similarities between plant and animal gametes. *Curr. Biol.* 20, 506–512. doi: 10.1016/j.cub.2010.01.051
- Wu, L. C., Wang, Z. W., Tsan, J. T., Spillman, M. A., Phung, A., Xu, X. L., et al. (1996). Identification of a RING protein that can interact *in vivo* with the BRCA1 gene product. *Nat. Genet.* 14, 430–440. doi: 10.1038/ng1296-430
- Yan, W., Shao, Z., Li, F., Niu, L., Shi, Y., Teng, M., et al. (2011). Structural basis of gammaH2AX recognition by human PTIP BRCT5-BRCT6 domains in the DNA damage response pathway. *FEBS Lett.* 585, 3874–3879. doi: 10.1016/j.febslet.2011.10.045
- Yan, S., Wang, W., Marqués, J., Mohan, R., Saleh, A., Durrant, W. E., et al. (2013). Salicylic acid activates DNA damage responses to potentiate plant immunity. *Mol. Cell* 52, 602–610. doi: 10.1016/j.molcel.2013.09.019
- Yoshiyama, K. O. (2016). SOG1: a master regulator of the DNA damage response in plants. *Genes Genet. Syst.* 90, 209–216. doi: 10.1266/ggs.15-00011
- Yoshiyama, K., Conklin, P. A., Huefner, N. D., and Britt, A. B. (2009). Suppressor of gamma response 1 (SOG1) encodes a putative transcription factor governing multiple responses to DNA damage. *Proc. Natl. Acad. Sci.* 106, 12843–12848. doi: 10.1073/pnas.0810304106

Yoshiyama, K., Kobayashi, J., Nobuo, O., Minako, U., Kimura, S., Maki, H., et al. (2013a). ATM-Mediated phosphorylation of SOG1 is essential for the DNA damage response in arabidopsis. *EMBO Rep.* 14, 817–822. doi: 10.1038/embor.2013.112

Yoshiyama, K. O., Sakaguchi, K., and Kimura, S. (2013b). DNA Damage response in plants: conserved and variable response compared to animals. *Biology* 2, 1338–1356. doi: 10.3390/biology2041338

Yu, X., Chini, C. C. S., He, M., Mer, G., and Chen, J. (2003). The BRCT domain is a phospho-protein binding domain. *Science* 302, 639–642. doi: 10.1126/science.1088753

Zhang, X., Henriques, R., Lin, S.-S., Niu, Q.-W., and Chua, N.-H. (2006). Agrobacterium-mediated transformation of arabidopsis thaliana using the floral dip method. *Nat. Protoc.* 1, 641–646. doi: 10.1038/nprot.2006.97